Research Square

Preprints are preliminary reports that have not undergone peer review.
They should not be considered conclusive, used to inform clinical practice,
or referenced by the media as validated information.

Dynamical Systems Modeling of Global Health Resource Allocation under Governance Constraints

Jean M. Tchuenche
University of the Witwatersrand
Jean Pierre II Kouenkam
kouenkus2@gmail.com
Université de Yaoundé I
Herieth Rwezaura
University of Dar es Salaam
Mamadou L. Diagne
Université de Thiès
Joseph Mbang
Université de Yaoundé I

Research Article

Keywords:

Posted Date: November 16th, 2026

DOI: https://doi.org/10.21203/rs.3.rs-11442331/v1

License: This work is licensed under a Creative Commons Attribution 4.0 International License.
Read Full License

Additional Declarations: No competing interests reported.

Dynamical Systems Modeling of Global Health Resource Allocation under Governance Constraints

Jean M. Tchuenche[1], Jean Pierre II Kouenkam[2]*, Herieth Rwezaura[3], Mamadou L. Diagne[4], Joseph Mbang[5,6]

[1]School of Computational and Applied Mathematics, University of the Witwatersrand, Johannesburg, South Africa

[2]Department of Renewable Energy, Faculty of Science, University of Yaounde I, Yaoundé, P.O. Box 812, Cameroon

[3] Mathematics Department, University of Dar es Salaam, Dar es Salaam, Tanzania

[4] Département de Mathématiques, Université Iba der Thiam de Thies, Thies, Sénégal

[5]Department of Mathematics, Faculty of Science, University of Yaounde I, Yaoundé, P.O. Box 812, Cameroon

[6] IRD UMI 209 UMMISCO, University of Yaounde I, Yaoundé, P.O. Box 337, Cameroon

LIRIMA, Project Team GRIMCAPE, Yaoundé, Cameroon

October 26, 2026

Abstract

Global health financing decisions must balance competing priorities: directing resources toward settings where they can generate the greatest service delivery, limiting fiduciary exposure, and ensuring that benefits are distributed equitably across populations. These objectives can conflict when implementation capacity differs across countries. A constrained multi-objective optimization model is developed to make these trade-offs explicit, linking financing flows to service delivery through country-specific efficiency parameters while incorporating fiduciary risk and inter-population inequality into the allocation problem. A social planner optimizes a weighted objective that balances

*Correspondence: kouenkus2@gmail.com

effective service delivery, risk mitigation, and distributional equity, allowing policy priorities to be represented explicitly through adjustable weights. A three-country numerical experiment illustrates how alternative policy priorities translate into different allocation outcomes. An efficiency-oriented allocation produces higher aggregate output ($Y = 79$), representing greater efficiency-adjusted service delivery, and lower fiduciary risk ($\mathcal{R} = 21$), but generates substantial disparities in per-capita benefits. An equity-oriented allocation reduces aggregate output ($Y = 69$) and increases fiduciary risk ($\mathcal{R} = 31$), but produces a more balanced distribution of benefits. These numerical examples are illustrative rather than empirical and are intended to make the model's trade-offs transparent and interpretable beyond a purely technical setting. The results demonstrate that efficiency, fiduciary risk, and equity cannot generally be optimized simultaneously, highlighting the importance of making allocation preferences explicit. The formulation provides a tractable basis for examining these trade-offs and a starting point for future extensions incorporating uncertainty, richer governance constraints, and empirical calibration.

Key Messages

- Global health resource allocation involves competing objectives: maximizing service delivery, limiting fiduciary risk, and promoting equitable distribution of benefits, particularly when implementation capacity differs across countries.
- Explicitly incorporating these objectives into a constrained allocation problem makes the efficiency–risk–equity trade-offs visible and shows how alternative policy priorities can produce substantially different allocation outcomes.
- The equity preference of the planner is a major determinant of distributional outcomes, while differences in implementation efficiency can substantially alter the allocation and the balance between aggregate performance and equity.
- Performance-based feedback can reinforce initial disparities by directing additional resources toward higher-performing settings; incorporating equity considerations into both allocation objectives and feedback rules may therefore be important when persistent distributional disparities are a policy concern.

1 Introduction

Programmatic solicitations in global health - spanning donor requests for proposals, implementation contracts, and market-shaping initiatives - implicitly define complex, multi-actor systems of financing, allocation, and service delivery. These systems are not static procurement instruments; rather, they operate as constrained, feedback-driven dynamical systems in which funding flows, institutional rules, and implementation capacity jointly determine population-level outcomes. Classical analytical approaches often decompose these layers, thereby limiting their ability to represent cross-layer feedback, governance constraints, and nonlinear performance effects that emerge from their interaction. Governance sets mean the set of allowable rules, policies, institutional constraints, or decision regimes that govern how the system can be controlled or operated.

In contrast, recent advances in control theory, network science, and operations research provide a natural foundation for representing such systems as governed multi-layer dynamical networks [1, 2, 3]. Within this perspective, programmatic health systems can be interpreted as interconnected dynamical processes evolving under structural constraints, information asymmetries, and policy-driven control rules. The paper develops model prototypes derived from programmatic solicitations to formalize global health financing and service-delivery architectures as constrained, multi-layer control systems with feedback. The formulation brings together inter-layer network dynamics, capacity-constrained allocation, governance-imposed control constraints, and adaptive feedback mechanisms, providing a mathematical representation of how financing architecture, implementation capacity, and governance interact to shape program performance and distributional outcomes. This perspective also permits explicit analysis of trade-offs among efficiency, fiduciary risk, and equity within a common allocation problem. The remainder of the paper develops this formulation and examines its behavior through illustrative numerical experiments, dynamic analysis, and sensitivity analysis. The numerical results are illustrative rather than empirical and are intended to make the model's trade-offs transparent and interpretable for policy and decision makers, as well as for technical and non-technical audiences.

The rest of the paper is organized as follows: Section 2 presents the governed four-layer dynamical architecture and formulates the associated governance-constrained optimization problem. Section 3 uses illustrative numerical examples to examine how alternative efficiency and equity priorities translate into different resource-allocation

patterns, the resulting planner's problem and efficiency–equity Pareto frontier, and how the allocation evolves over time under performance-based feedback and exogenous shocks. Section 4 assesses how the optimal allocation changes with the equity weight and characterizes distinct allocation regimes through a phase diagram, followed by Morris and Sobol global sensitivity analyses. Section 5 synthesizes the main findings, discusses the model's limitations and directions for future development, and considers their implications for policy. Section 6 concludes the paper by highlighting the main contributions and implications for allocation decisions under competing efficiency, risk, and equity objectives.

2 Model Formulation: Governed Four-Layer Dynamical Architecture

Programmatic health systems can be represented as interconnected dynamical processes evolving under structural constraints, information asymmetries, and policy-driven control rules. The model prototypes developed here are derived from the institutional and financing structures represented in programmatic solicitations and formalize global health financing and service-delivery architectures as constrained, multi-layer control systems with feedback. The formulation integrates: (i) inter-layer network dynamics capturing interactions among donors, implementing agencies, and service-delivery systems; (ii) capacity-constrained allocation and implementation processes formulated as optimization problems subject to feasibility restrictions [4]; (iii) governance-imposed control constraints reflecting procurement rules, accountability requirements, and regulatory oversight; and (iv) closed-loop feedback mechanisms through which observed performance, cross-country interactions, and external shocks affect subsequent system behavior. This formulation is consistent with system-level conceptualizations of health systems as interconnected institutional and operational components subject to endogenous feedbacks and structural constraints [5]. It provides a basis for examining how governance design, financing architecture, and implementation capacity jointly shape performance, efficiency, fiduciary risk, and equity outcomes. The abstraction from programmatic solicitations into the mathematical system involves several complementary components representing financial flows, institutional relationships, implementation capacity, service delivery, and population-level outcomes, as illustrated in Figure 1.

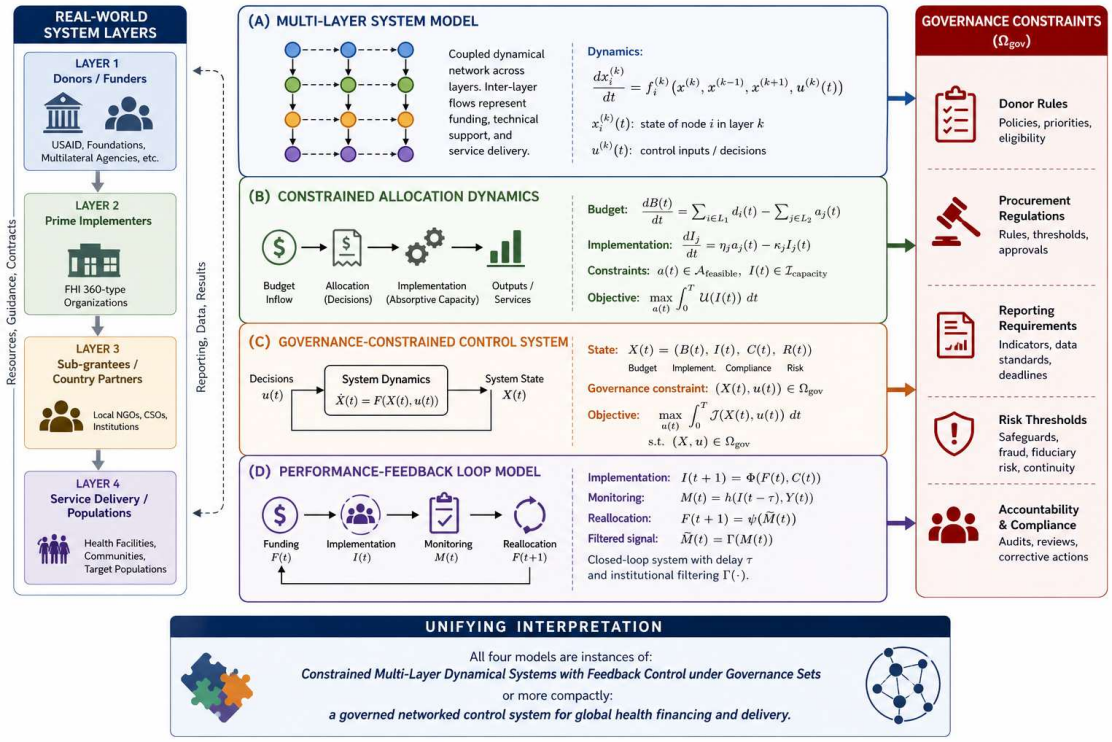


Figure 1: Simplified flow diagram of model prototypes derived from programmatic solicitations.

The resulting system incorporates several feedback and response mechanisms that connect the different institutional layers. First, an upward feedback mechanism operates through performance-dependent funding, whereby realized country-level outcomes influence subsequent donor allocation decisions. Second, a horizontal feedback mechanism captures cross-country learning and diffusion of implementation practices among executing entities, allowing information and operational strategies to propagate across the system. Third, a downward feedback mechanism represents the influence of donor priorities, conditionalities, and strategic objectives on implementation behavior and operational decisions at the delivery level. Finally, an exogenous-shock mechanism represents disruptions such as conflict, epidemic outbreaks, inflationary pressures, or supply-chain interruptions that perturb financing flows, implementation capacity, and service-delivery outcomes.

2.1 The model

Large-scale development and global health programs are rarely implemented through a single institution. Instead, they operate through multi-tier financing and delivery chains in which resources originate from donors, pass through prime implementers, are redistributed to country partners, and ultimately generate outcomes at the service-delivery level. Examples include the Global Fund, Gavi, USAID, and PEPFAR. Quantitative models commonly focus on individual components of these systems, such as financing flows, epidemiological or service-delivery outcomes, or single-agent optimization. The formulation developed here instead connects these components within a four-layer governed dynamical network linking financing, institutions, delivery systems, and outcomes.

Define the programmatic system as a coupled multilayer network as depicted in Figure 1:

$$\mathcal{G} = (\mathcal{L}_1, \mathcal{L}_2, \mathcal{L}_3, \mathcal{L}_4, \mathcal{E}), \tag{1}$$

where:

- $\mathcal{L}_1$: Donors / Funders (bilateral agencies, philanthropic foundations, multilateral institutions),
- $\mathcal{L}_2$: Prime implementers (international NGOs, UN agencies, technical consortia),
- $\mathcal{L}_3$: Sub-grantees / Country partners (ministries, local NGOs, district systems),
- $\mathcal{L}_4$: Service delivery / Target populations (clinics, communities, beneficiaries),
- $\mathcal{E}$: Directed weighted edges representing transfers of funds, commodities, information, reporting obligations, and accountability constraints.

Let $F_i(t)$ denote the financial resources available, $C_i(t)$ the operational or absorptive capacity, $Q_i(t)$ the quality/performance index, and $R_i(t)$ the compliance/reporting score. Then, each node i in layer k possesses a time-dependent state vector:

$$x_i^{(k)}(t) = \begin{bmatrix} F_i(t) \\ C_i(t) \\ Q_i(t) \\ R_i(t) \end{bmatrix}. \tag{2}$$

Hence, each actor is characterized not only by funding, but also by institutional readiness and governance quality. For the interlayer flow dynamics, assume that financial resources evolve according to

$$\dot{F}_j(t) = \sum_i a_{ij} u_{ij}(t) - \delta_j F_j(t), \tag{3}$$

where a_{ij} denotes connectivity from node i to node j, $u_{ij}(t)$ is the transfer or allocation control, δ_j is the leakage, delay, or administrative loss rate. Operational capacity evolves through investment and learning

$$\dot{C}_j(t) = \alpha_j F_j(t) - \beta_j C_j(t) + \eta_j, \tag{4}$$

where α_j measures funding-to-capacity conversion, β_j depreciation, and η_j exogenous support. Service quality satisfies:

$$Q_j(t) = g(F_j(t), C_j(t), R_j(t)) \,. \tag{5}$$

Population-level outcomes are generated through Layer 4 performance as

$$Y(t) = h\left(\sum_{j \in \mathcal{L}_4} Q_j(t) \right), \tag{6}$$

where $Y(t)$ may represent vaccination coverage, treatment completion, mortality reduction, or service reach.

2.2 Governance-constrained optimization

Decision makers seek to maximize programmatic impact while penalizing financial, operational, and distributional failures over the planning horizon:

$$\max_{u(t) \in \mathcal{U}} \int_0^T \left[\omega_1 Y(t) - \omega_2 \mathcal{R}(t) - \omega_3 \mathcal{I}(t) \right] dt, \tag{7}$$

where $Y(t)$ denotes aggregate health or development impact at time t (e.g., treatment success, service coverage, mortality reduction, beneficiaries reached), $\mathcal{R}(t)$ is a composite risk functional capturing fiduciary, operational, and implementation vulnerabilities, $\mathcal{I}(t)$ is an inequity functional measuring unequal allocation of resources or outcomes across countries, regions, or target populations, $\omega_1, \omega_2, \omega_3 > 0$ are policy weights reflecting the planner's priorities.

Let $R_f(t)$ denote the financial misuse or leakage risk, $R_d(t)$ the implementation delay risk, $R_c(t)$ the complianc or reporting failure risk, and $R_s(t)$ the supply-chain disruption or stockout risk. A convenient decomposition of total risk is given by

$$\mathcal{R}(t) = \lambda_1 R_f(t) + \lambda_2 R_d(t) + \lambda_3 R_c(t) + \lambda_4 R_s(t), \tag{8}$$

where $\lambda_i \geq 0$ represents the severity weights. For example,

$$R_f(t) = \sum_j \rho_j F_j(t)\, \phi\big(1 - R_j(t)\big), \tag{9}$$

so that entities receiving large funds with weak compliance scores generate higher fiduciary risk. $\rho_j \geq 0$ denotes an entity-specific fiduciary risk exposure parameter capturing structural vulnerability and governance sensitivity associated with channel j. The function $\phi(\cdot)$ represents a nonlinear risk transformation and can take various functional forms depending on the assumed risk response structure, e.g., Linear: $\phi(x) = x$, Convex amplification: $\phi(x) = x^2$, Threshold effects: $\phi(x) = \mathbf{1}_{x>\tau}$, Saturation: $\phi(x) = 1 - e^{-x}$. Similarly,

$$R_d(t) = \sum_j \max\{0, \tau_j(t) - \tau_j^*\}, \tag{10}$$

where $\tau_j(t)$ is realized implementation delay and τ_j^* is the target completion time.

Let g indexes countries, districts, or vulnerable groups, $y_g(t)$ is benefit delivered to group g, and N_g is the population size of group g. The inequity term may be defined as

$$\mathcal{I}(t) = \sum_{g=1}^{G} \left(\frac{y_g(t)}{N_g} - \frac{Y(t)}{\sum_{h=1}^{G} N_h} \right)^2, \tag{11}$$

This inequity measure (which is a population-weighted squared deviation from the global mean) belongs to the class of variance-based inequality indices and can be interpreted as a quadratic between-group deviation from the population mean, closely related to generalized entropy and squared coefficient-of-variation measures used in inequality decomposition. Thus, $\mathcal{I}(t)$ penalizes disparities in per-capita outcomes across groups. Alternative inequity measures from the economics and operations research literature may also be incorporated into the planner objective:

- **Gini coefficient**, a classical measure of dispersion in the distribution of income, resources, or outcomes [32, 10];

- **Atkinson index**, which embeds explicit aversion to inequality through a welfare parameter [30];
- **Theil index**, an entropy-based inequality measure that is decomposable across subgroups [31, 13];
- **Max-min fairness**, which prioritizes the least-served group before allocating additional gains elsewhere [28, 15];
- **Nash social welfare**, balancing efficiency and fairness through the product (or sum of logs) of group utilities [16, 17];
- **Proportional fairness**, widely used in network resource allocation and congestion control [29].

These metrics allow policymakers to formalize ethical or operational preferences regarding equity in service coverage, funding distribution, or health outcomes. Hence, the planner chooses controls $u(t)$ (funding allocations, contracts, procurement schedules, technical support, reallocations) to maximize impact while minimizing corruption risk, delivery failures, and unequal access.

The proposed model is supported by a structured set of state variables and parameters that characterize the dynamics of financing, implementation, governance, and population-level outcomes within a multi-layer global health system. Table 1 summarizes the state variables describing the evolution of financial resources, operational capacity, implementation quality, governance and compliance, funding allocations, implementation levels, monitoring indicators, fiduciary and operational risks, equity measures, and aggregate program outcomes. Collectively, these variables capture the interactions among donor financing, institutional capacity, governance constraints, implementation performance, and adaptive feedback mechanisms that determine the effectiveness and sustainability of global health investments. Table 2 presents the corresponding model parameters governing resource flows, capacity accumulation, implementation efficiency, administrative losses, fiduciary risk, governance constraints, monitoring dynamics, and planner preferences within the optimization framework. Where available, parameter ranges are informed by the health systems, global health financing, and operations research literature, while policy weights and decision functions are specified by the planner to reflect alternative strategic priorities. Together, these variables and parameters define the temporal scales, institutional interactions, and optimization tradeoffs underlying the governed multi-layer resource allocation framework, providing a rigorous foundation for analyzing efficiency, equity, resilience,

Variable	Description
$F_i(t)$	Financial resources available to institution i
$C_i(t)$	Operational (absorptive) capacity of institution i
$Q_i(t)$	Implementation quality or performance index
$R_i(t)$	Governance and compliance score
$Y(t)$	Aggregate health or development outcome
$B(t)$	Total available donor budget
$I_j(t)$	Implementation level of implementing partner j
$u_{ij}(t)$	Funding transfer from institution i to institution j
$a_j(t)$	Allocation to implementing partner j
$d_i(t)$	Donor funding inflow
$\mathcal{R}(t)$	Composite fiduciary and operational risk index
$\mathcal{I}(t)$	Equity (inequality) penalty function
$R_f(t)$	Financial misuse (fiduciary) risk
$R_d(t)$	Implementation delay risk
$R_c(t)$	Compliance/reporting risk
$R_s(t)$	Supply-chain disruption risk
$y_g(t)$	Effective services delivered to population group g
N_g	Population size of group g
$X(t)$	Complete system state vector (B, I, C, R)
$M(t)$	Monitoring and evaluation performance indicator
$\tilde{M}(t)$	Filtered monitoring information
$\Omega_{\text{governance}}$	Governance-constrained feasible decision set

Table 1: Description of state variables used in the governed multi-layer global health financing framework.

and governance in complex global health financing systems. Numerical results below are illustrative rather than empirical and are intended to make the model's trade-offs transparent and interpretable for policy and decision makers, as well as for technical and non-technical audiences.

3 Illustrative examples

To illustrate the behavior of the planner's optimization problem, a stylized single-period allocation model is considered for three countries. The example shows how alternative policy priorities interact with differences in implementation efficiency under a constrained budget, and how these choices affect aggregate service delivery,

Parameter	Description	Value/Range	Source
α_j	Funding-to-capacity conversion rate	0.4-0.9	[19, 20]
β_j	Capacity depreciation rate	0.02-0.15 month^{-1}	[19]
δ_j	Administrative leakage/loss rate	0.01-0.10	[21]
η_j	External technical assistance coefficient	0-0.30	[23]
κ_j	Implementation efficiency	0.40-0.95	[22, 20]
ρ_j	Fiduciary risk coefficient	0.10-1.00	[21]
λ_1	Weight for fiduciary risk	$0-1$	Policy dependent
λ_2	Weight for implementation delay	$0-1$	Policy dependent
λ_3	Weight for compliance risk	$0-1$	Policy dependent
λ_4	Weight for supply-chain risk	$0-1$	Policy dependent
ω_1	Weight on program impact	1 (baseline)	Planner preference
ω_2	Weight on risk penalty	0.5 (illustrative)	Planner preference
ω_3	Weight on equity penalty	50 (illustrative)	Planner preference
a_{ij}	Network connectivity weight	$0-1$	[26, 27]
τ_j^*	Target implementation time	6-24 months	[23]
$\Gamma(\cdot)$	Monitoring/filtering operator	Dimensionless	[25]
$\Phi(\cdot)$	Implementation response function	Dimensionless	[25]
$\psi(\cdot)$	Performance-based funding function	Dimensionless	[22]
$\pi_j(\cdot)$	Allocation decision function	Dimensionless	[24]

Table 2: Summary of model parameters used in the governed multi-layer optimization framework for global health financing. Parameter values are representative ranges reported in the health systems, operations research, and global health financing literature or are policy-dependent weights selected by the decision-maker.

fiduciary risk, and the distribution of benefits across countries.

3.1 Problem setup

Let the decision vector be

$$u = (u_1, u_2, u_3),$$

where $u_g \geq 0$ denotes the funding allocated to country $g \in \{1, 2, 3\}$. The total budget constraint is given by

$$\sum_{g=1}^{3} u_g = 100, \quad \text{(million monetary units)}.$$

Countries are characterized by population sizes

$$N = (10,\ 20,\ 30) \quad (N_g \text{ in million}),$$

and implementation efficiency parameters

$$\kappa = (0.90,\ 0.70,\ 0.50), \quad \kappa_g \in (0, 1].$$

We adopt a linear production technology in which funding is converted into effective service delivery according to

$$y_g = \kappa_g u_g,$$

so that total system-wide output is

$$Y = \sum_{g=1}^{3} y_g.$$

Fiduciary and operational risk is modeled as an increasing function of low-capacity allocation:

$$\mathcal{R} = \sum_{g=1}^{3} (1 - \kappa_g) u_g,$$

while inequity is measured via dispersion in per-capita benefits:

$$\mathcal{I} = \sum_{g=1}^{3} \left(\frac{y_g}{N_g} - \frac{Y}{\sum_{h=1}^{3} N_h} \right)^2.$$

Now, we take into account two scenarios: the first is an allocation favoring high-implementation efficiency and the second consider a more balanced allocation:

Scenario A: Efficiency-biased allocation

$$u = (60,\ 25,\ 15).$$

The *efficiency*' allocation concentrates resources on Country 1. The resulting outputs are:

$$y = (54,\ 17.5,\ 7.5), \quad Y = 79.$$

The corresponding risk level is:

$$\mathcal{R} = 0.1(60) + 0.3(25) + 0.5(15) = 21,$$

Moreover, per-capita benefits are:

$$(5.40,\ 0.875,\ 0.25)\,,$$

indicating substantial disparity across countries. The corresponding value of inequity is $\mathcal{I} = 18.0065$.

Scenario B: Equity-biased allocation

$$u = (30,\ 35,\ 35).$$

The *equity* allocation brings the three countries closer to an equal split. The resulting outputs are:

$$y = (27,\ 24.5,\ 17.5), \quad Y = 69.$$

The risk level increases to:

$$\mathcal{R} = 0.1(30) + 0.3(35) + 0.5(35) = 31.$$

In addition, per-capita benefits are:

$$(2.70,\ 1.225,\ 0.583)\,,$$

which exhibit substantially reduced inequality ($\mathcal{I} = 2.7292$) relative to Scenario A.

Summary comparison

Scenario	Total Output Y	Risk $\mathcal{R}$	Equity (dispersion)
A: Efficiency-biased	79	21	Low equity
B: Equity-biased	69	31	Higher equity

The numerical experiment highlights a fundamental tradeoff in constrained global health allocation systems. Efficiency-oriented allocations maximize aggregate service delivery but exacerbate inequality across population groups. Conversely, equity-oriented allocations improve distributional fairness at the cost of reduced aggregate output and increased exposure to low-capacity implementation channels.

3.2 Planner's problem

Policy- and decision-makers are often interested in the allocation problem faced by a social planner, who seeks to balance efficiency, fiduciary risk, and equity. Formally, the planner solves:

$$\max_{u} \left[\omega_1 Y - \omega_2 \mathcal{R} - \omega_3 \mathcal{I}\right], \tag{12}$$

subject to budget feasibility, where the weights are specified as

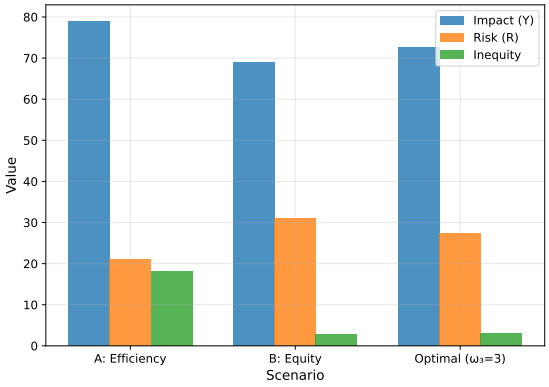
$$\omega_1 = 1, \quad \omega_2 = 0.5, \quad \omega_3 = 3.$$

The weighting parameters $\omega_1, \omega_2, \omega_3$ determine the relative emphasis placed on efficiency, fiduciary risk, and equity, thereby tracing a continuum of optimal funding

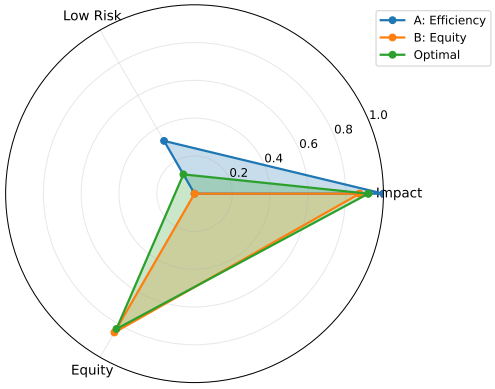
strategies that correspond to different institutional objectives. Figure 2 contrasts Scenarios A (efficiency-biased allocation) and B (equity-biased allocation) with the optimal allocation obtained by explicitly solving the planner's problem. The comparison is presented from complementary perspectives: aggregate outcomes in terms of $Y, \mathcal{R}, \mathcal{I}$, depicted in Figure 2(a); the normalized multi-objective trade-off across competing objectives, shown as a radar chart in Figure 2(b); country-level allocation patterns, depicted in Figure 2(c); and, finally, the resulting per-capita benefits, depicted in Figure 2(d).

Figure 2(a) quantifies the trade-off achieved by the planner's optimal allocation. The optimum attains an impact of $Y \approx 73$, approaching Scenario A ($Y = 79$), while substantially reducing inequity relative to the efficiency-biased allocation. This improvement in equity is achieved with an intermediate fiduciary risk of $\mathcal{R} \approx 23$, between the values of 21 and 31 observed under the two reference scenarios. The radar chart (Figure 2(b)) provides a visual representation of this multi-objective trade-off, showing that the planner's optimal allocation combines high impact, relatively low fiduciary risk, and greater equity in a configuration that is not captured by either polar scenario alone. These results illustrate the value of explicitly solving the optimization problem: rather than choosing between efficiency- and equity-biased allocations, the planner's solution identifies an intermediate allocation that balances the competing objectives.

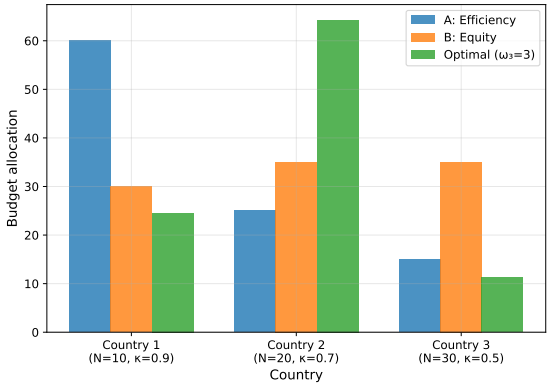
It should be noted that, although $\omega_3 = 3$ yields a compromise across the competing objectives, the resulting optimal solution remains closer to Scenario A than to Scenario B. Indeed, Figure 2(c) shows that more than half of the available resources are allocated to Country 2, which has an efficiency of 0.7. Consequently, as shown in Figure 2(d), the optimal allocation substantially improves the per-capita benefit for Country 2, while the corresponding benefit for Country 3 remains close to that observed under Scenario A. This allocation pattern is consistent with the still-moderate weight assigned to equity through $\omega_3 = 3$, which allows efficiency considerations to remain influential while introducing a measurable equity-oriented adjustment.



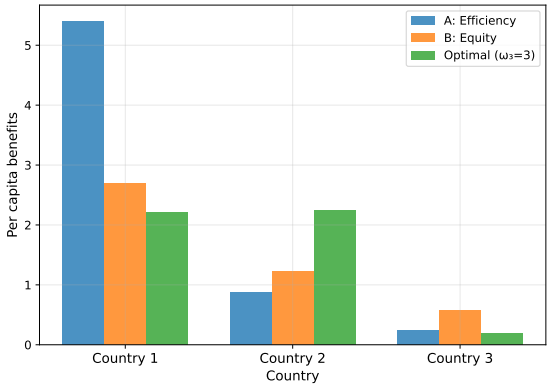
(a) Metrics comparison.



(b) Normalized multi-objective trade-off.



(c) allocation comparison.



(d) per-capita benefits distribution.

Figure 2: Comparison of the three scenarios.

3.3 Efficiency-equity Pareto frontier

Figure 3 traces the complete Pareto frontier obtained by varying ω_3 over a fine grid while keeping $\omega_1 = 1$ and $\omega_2 = 0.5$ fixed, with fiduciary risk $\mathcal{R}$ encoded by color. The frontier exhibits a characteristic concave shape, revealing a clear asymmetry in the trade-off between impact and equity. Initial gains in impact, from $\mathcal{I} \approx 0$ to $\mathcal{I} \approx 5$, require only a modest sacrifice in equity. Beyond $\mathcal{I} \approx 10$, however, each additional gain in impact requires an increasingly large deterioration in equity, culminating in a plateau where impact approaches $Y \approx 90$ despite very high inequity ($\mathcal{I} > 50$). This plateau arises because the allocation becomes increasingly concentrated in Coun-

try 1, after which the budget constraint leaves little scope for further improvement in Y.

The color gradient further reveals a systematic relationship between the equity–impact trade-off and fiduciary risk. High-inequity points (yellow, $\mathcal{R} \approx 10$) correspond to allocations concentrated in the most efficient country and therefore entail the lowest fiduciary risk, whereas low-inequity points (purple, $\mathcal{R} \approx 30$) correspond to allocations that distribute resources more broadly across less efficient channels. Scenarios A and B lie visibly *under* the frontier, whereas the planner's optimal allocation lies *exactly on* the frontier. This provides numerical confirmation that, for the specified objective weights, the planner's solution is Pareto-efficient: no improvement in one objective can be achieved without sacrificing at least one of the competing objectives.

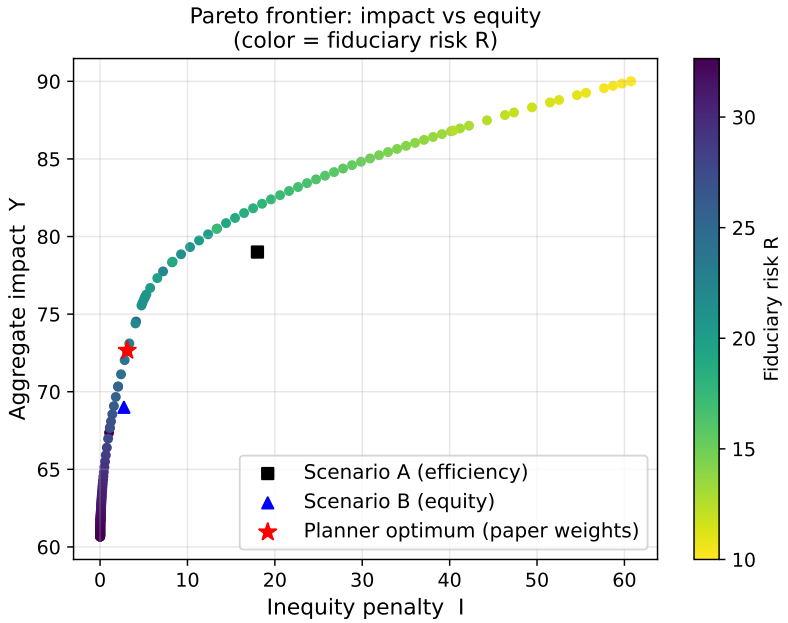


Figure 3: Pareto frontier of impact (Y) versus inequity ($\mathcal{I}$), colored by fiduciary risk ($\mathcal{R}$). Scenarios A, B and the planner's optimum (paper weights) are overlaid.

3.4 Feedback dynamics and response to an exogenous shock

The proposed framework is illustrated using the same three-country synthetic system with population vector

$$N = (10,\ 20,\ 30), \quad \kappa = (0.90,\ 0.70,\ 0.50), \quad u_1 + u_2 + u_3 = 100.$$

For the baseline donor allocation and implementation layer, consider the efficiency-oriented allocation

$$u^0 = (60,\ 25,\ 15).$$

Recall that the country-level effective service delivery is given by

$$y_g^0 = \kappa_g u_g^0, \quad y^0 = (54,\ 17.5,\ 7.5), \quad Y^0 = 79.$$

For the governance and compliance layer, fiduciary exposure is computed as

$$\mathcal{R}^0 = \sum_{g=1}^{3} (1 - \kappa_g) u_g^0 = 21,$$

And for the population outcome layer, the per-capita effective service delivery is

$$(5.40,\ 0.875,\ 0.25),$$

indicating substantial inter-country dispersion in realized outcomes.

3.4.1 Feedback dynamics

For the feedback layer (donor response), assume an upward feedback rule in which future allocations adjust according to performance:

$$u_g(t+1) = u_g(t) + \eta \left(\frac{y_g(t)}{N_g} - \bar{y}(t) \right), \quad \eta = 2,$$

where after t periods, for country g, $g \in \{1, 2, 3\}$, $u_g(t)$ and $y_g(t)$ respectively denote the funding allocated and the effective services delivered to population, while $\bar{y}(t)$ stands for the mean per-capita outcome of all countries taken together. This induces a reallocation of resources toward higher-performing countries in subsequent cycles.

Figure 4 shows that the feedback rule converges, in free running (no shock), toward a *total* concentration of the budget on Country 1 within about ten periods. As a matter of fact, once Country 1 exhibits an above-average per-capita benefit,

the feedback rule keeps transferring resources to it. This trend further increases the relative advantage of Country 1: a self-reinforcing cumulative effect (*winner-take-all*) rather than a rebalancing. This illustrates an important limitation of purely performance-driven feedback: without an explicit equity counterweight (such as the $\mathcal{I}$ term in the planner's objective), it structurally tends to amplify initial gaps rather than correct them.

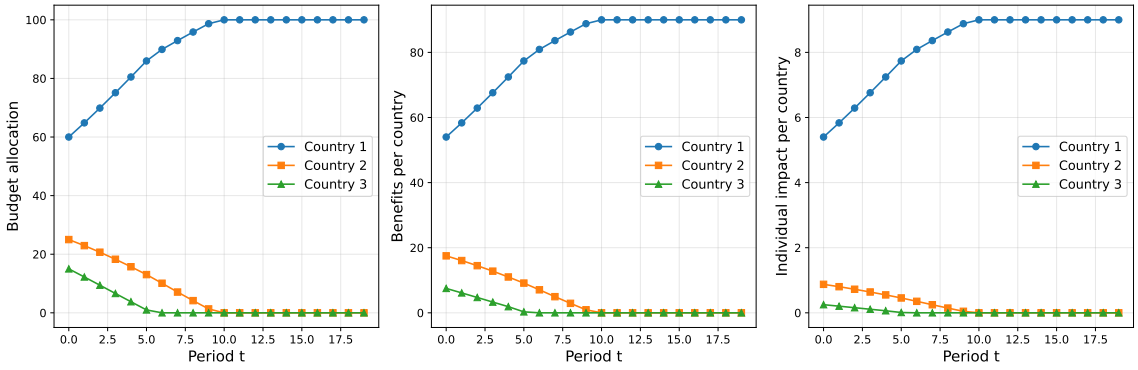


Figure 4: Effect of the performance-based feedback rule: budget allocation (left), benefits by country (center), and individual impact by country (right), as a function of period t.

3.4.2 Response to an exogenous shock

Consider a shock (system perturbation) occuring after s periods and affecting Country 3 (for example, a supply-chain disruption), reducing its efficiency from

$$\kappa_3 = 0.50 \to 0.30.$$

Holding u^0 fixed, outputs become

$$y^s = (54,\ 17.5,\ 4.5), \quad Y^s = 76.$$

Fiduciary exposure increases to

$$\mathcal{R}^s = 0.1(60) + 0.3(25) + 0.7(15) = 24.$$

Furthermore, consider that after the schock, a counterfactual direct-financing strategy reallocates funds toward higher-capacity systems as follows:

$$u^d = (70,\ 20,\ 10).$$

Then, the associated values of the country-level effective service delivery and the fiduciary exposure are respectively:

$$Y^d = 63 + 14 + 5 = 82 \qquad \text{and} \qquad \mathcal{R}^d = 19.$$

Figure 5 compares the responses of the three strategies – static, feedback, direct funding – to the shock affecting Country 3 at $t = 5$. It highlights three clearly differentiated response regimes.

- The *baseline* strategy (fixed allocation) absorbs the shock passively: $Y(t)$ drops instantaneously from 79 to 76 at $t = 5$ and remains flat thereafter, with the system never recovering: a direct illustration of the vulnerability of static financing to exogenous disruptions.

- The *contractual direct-funding* strategy reacts instantaneously to the shock (reallocation to $u^d = (70, 20, 10)$ at $t = 5$) and immediately stabilizes the system at a level above the baseline ($Y \approx 80$, $\mathcal{R} \approx 20$), and also above its own pre-shock value, which is consistent with the fact that this reallocation simultaneously corrects an inefficiency already present in u^0.

- The *performance-based feedback* strategy, by contrast, highlights the progressive concentration phenomenon already observed in Figure 4: $Y(t)$ continues to grow well after the shock, converging to a high plateau ($Y \to 90$) within about ten periods, at the cost of an inequity that explodes in parallel ($\mathcal{I}(t)$ exceeds 60, far above the other two strategies). This contrast illustrates a fundamental dynamic trade-off: pure feedback maximizes long-run impact but at the cost of structurally growing inequity, while contractual direct funding offers a more balanced trade-off and a faster reaction, without converging to extreme concentration.

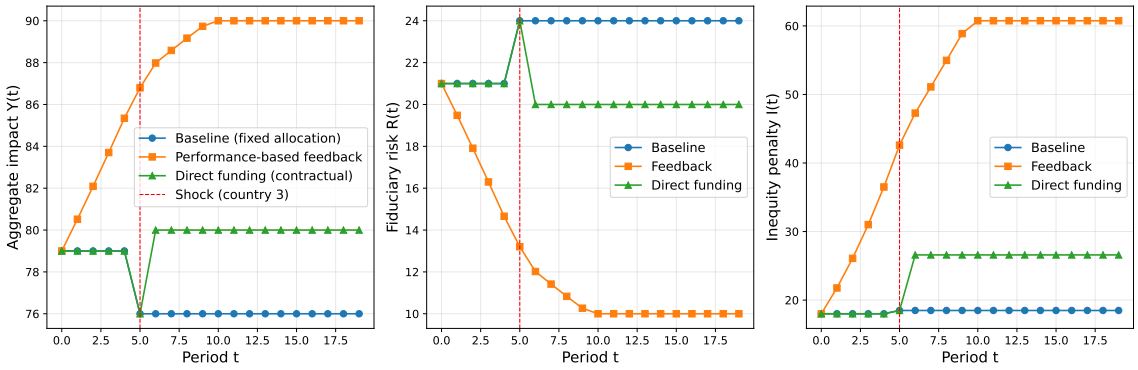


Figure 5: Dynamic response of the system to a shock affecting Country 3 at $t = 5$ ($\kappa_3 : 0.50 \to 0.30$), under three strategies: fixed allocation (*baseline*), performance-based feedback, and contractual direct funding. From left to right: aggregate impact $Y(t)$, fiduciary risk $\mathcal{R}(t)$, inequity penalty $\mathcal{I}(t)$.

4 Sensitivity Analysis

4.1 Local sensitivity of the optimal allocation to the equity weight

Figure 6 (left panel) reveals an instructive, non-monotonic reallocation dynamic as the equity weight ω_3 increases. For very low ω_3, the entire budget is concentrated on Country 1 ($u_1^* \to 100$). Once ω_3 exceeds a critical threshold of approximately $\omega_3 \approx 2$, Country 2 temporarily becomes the main beneficiary, with u_2^* reaching a local maximum close to 70, before gradually stabilizing. Thus, the planner does not switch directly from the most efficient to the least efficient country as the equity objective gains importance. Instead, the allocation initially favors the *intermediate* country, which provides a favorable balance between efficiency and need. Only from approximately $\omega_3 \approx 10$ does Country 3 receive substantial additional funding. At higher values of ω_3, the three allocations converge toward an asymptotic plateau of approximately $u^* \to (11, 30, 59)$ beyond $\omega_3 \approx 30$. This stabilization indicates that further increases in the equity weight produce little additional redistribution once the allocation has approached the equity-oriented limit permitted by the budget constraint.

Furthermore, the right panel reinforces this interpretation. $\mathcal{I}^*$ falls sharply with the initial increases in ω_3, declining from approximately 61 to almost 0 by $\omega_3 \approx 5$,

while Y^* decreases correspondingly before stabilizing. In contrast, $\mathcal{R}^*$ increases as the allocation becomes more broadly distributed. The resulting pattern–a rapid reduction in inequity followed by a plateau–shows that a substantial portion of the attainable equity gain occurs at relatively modest values of ω_3, whereas increases beyond $\omega_3 \approx 30$ produce comparatively little additional change in the allocation or equity outcome. This sensitivity analysis therefore identifies a region in which the equity objective has a pronounced effect on resource allocation without requiring the very high values of ω_3 that generate diminishing marginal changes in the solution.

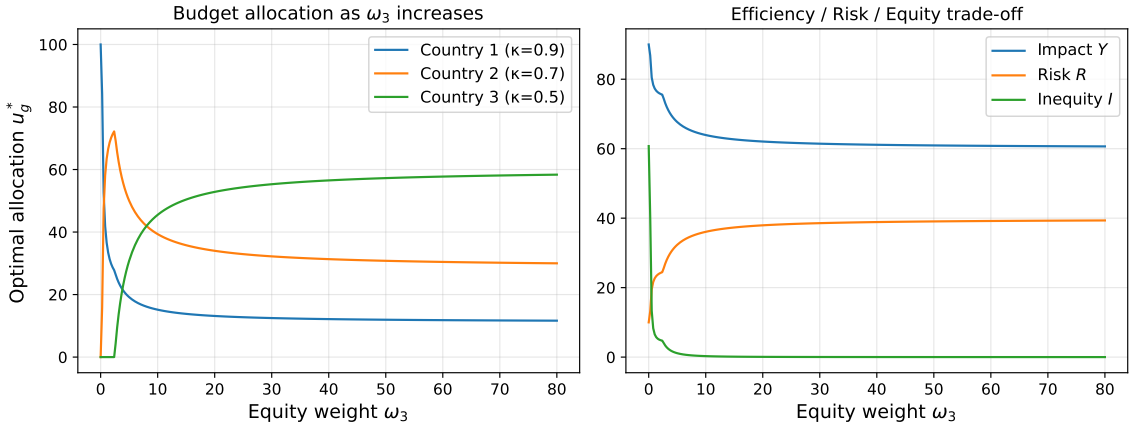


Figure 6: Optimal allocation u_g^* by country as a function of the equity weight ω_3 (left). Corresponding values of $Y^*, \mathcal{R}^*, \mathcal{I}^*$ at the optimum (right).

4.2 Phase diagram of optimal allocation regimes

Figure 7 illustrates, over the grid $(\omega_2, \omega_3) \in [0, 2] \times [0, 50]$, the dominant optimal allocation regimes across different combinations of the risk weight (ω_2) and the equity weight (ω_3). Specifically, the diagram identifies the country receiving the largest budget share under each parameter configuration. The parameter κ represents country-specific characteristics, with Country 1 ($\kappa = 0.90$), Country 2 ($\kappa = 0.70$), and Country 3 ($\kappa = 0.50$) representing progressively lower values of this attribute. Across the explored parameter space, the allocation pattern indicates that countries with lower κ values tend to become dominant as greater weight is placed on equity.

The phase diagram reveals three distinct allocation regimes. Country 3, represented in gray, occupies the largest region of the parameter space. In particular, for high ω_3 (above approximately 15), Country 3 dominates across the full range $\omega_2 \in [0, 2]$, indi-

cating that sufficiently strong equity weighting consistently shifts the largest budget share toward this country. At the lower boundary of the map ($\omega_3 \lesssim 15$), Country 2, shown in light green, occupies an intermediate region that expands as the risk weight ω_2 increases, producing a step-wise progression of the regime boundary. Country 1, depicted in teal, remains dominant only within a narrow band at very low equity weights ($\omega_3 < 2$), with relatively little dependence on ω_2. This pattern is consistent with the transient peak in u_2^* observed in Figure 6.

Two main observations emerge from this phase diagram. First, within the explored range, the dominant allocation regime is driven primarily by the equity weight ω_3, whereas changes in the risk weight ω_2 mainly affect the boundary between the intermediate regimes. Second, Country 1, despite having the highest κ and corresponding efficiency advantage, dominates only when the equity weight is very low. As ω_3 increases, the optimal allocation progressively shifts toward countries with lower κ, with Country 2 emerging as an intermediate regime before Country 3 becomes dominant. Thus, the phase diagram identifies ω_3 as the principal parameter governing transitions between dominant allocation regimes, while ω_2 modulates the location of these transitions over the explored range.

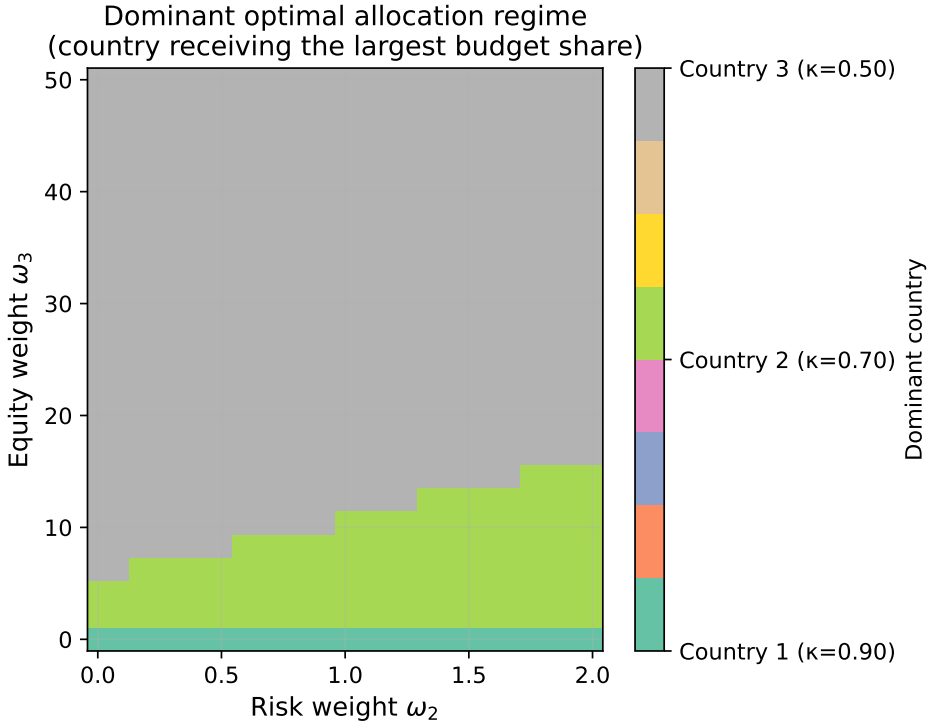


Figure 7: Dominant optimal allocation regime (country receiving the largest budget share) as a function of the risk weight ω_2 and the equity weight ω_3.

4.3 Global sensitivity analysis: Morris and Sobol results

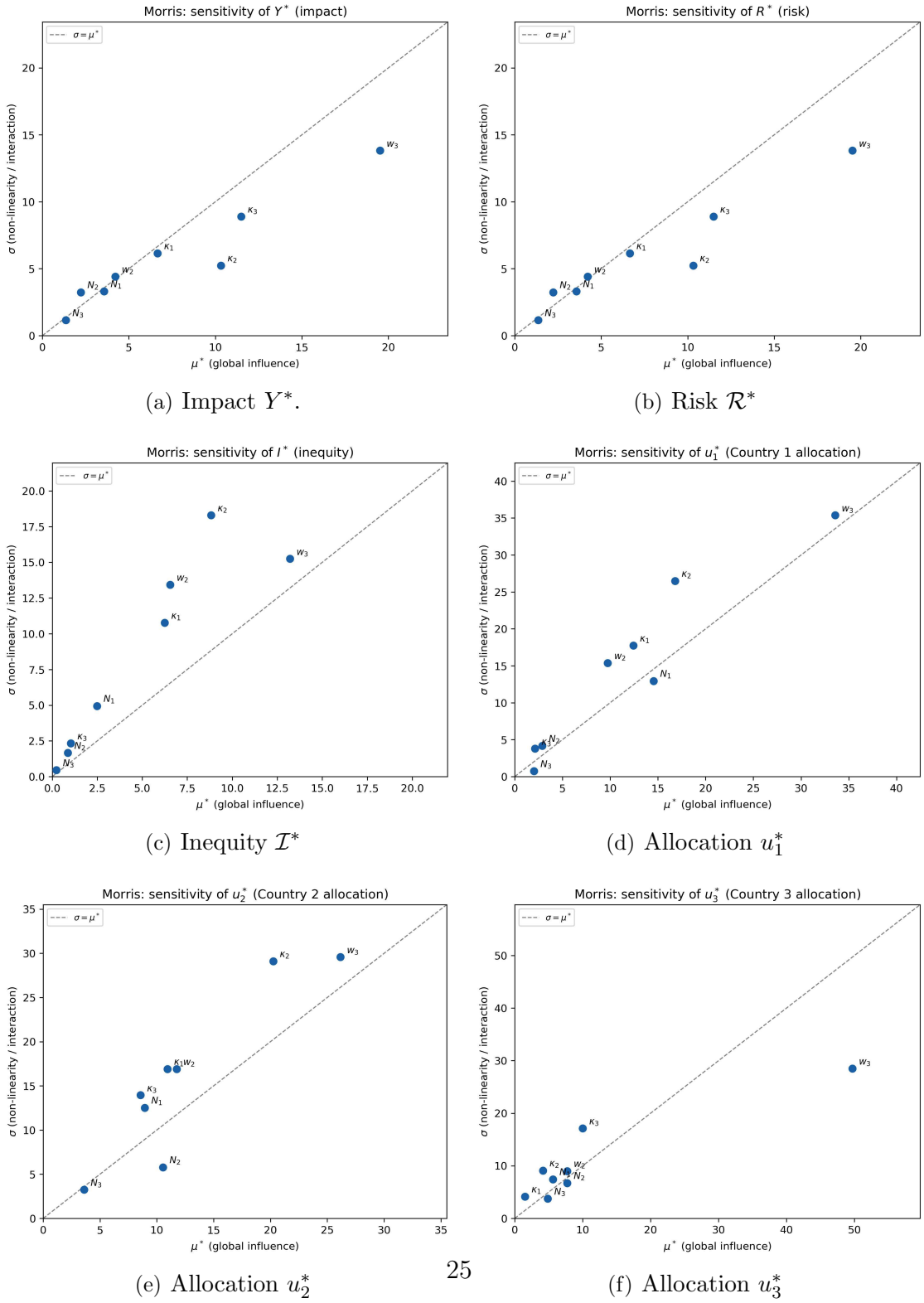
The global sensitivity analysis is conducted using two complementary methods: the Morris screening procedure [33, 34, 35], which identifies influential parameters and detects non-linearities or interactions, and the Sobol variance decomposition [36, 37, 38], which quantifies the share of output variance attributable to each parameter and to interactions. Eight parameters are subjected to screening: the three efficiencies $\kappa_1, \kappa_2, \kappa_3$ (ranges $\pm$15-20% around nominal values), the three populations N_1, N_2, N_3 (ranges $\pm$20%), and the policy weights ω_2, ω_3 ($\omega_1 = 1$ remaining the fixed reference, since only the ratios $\frac{\omega_2}{\omega_1}$, and $\frac{\omega_3}{\omega_1}$ determine the optimal allocation). Twelve diagnostics are produced: six Morris diagrams ($\mu^* - \sigma$ planes), where μ^*, the mean of the absolute elementary effects, measures the overall magnitude of a parameter's influence, while σ, the standard deviation of the elementary effects, captures their variability across the sampled parameter space, reflecting potential nonlinearities and interactions [39], and six Sobol spectra (S_1 and S_T indices), one for each output of

interest $(\mathcal{I}, \mathcal{R}, u_1^*, u_2^*, u_3^*, Y^*)$. The Morris screening was performed with $r = 70$ trajectories, corresponding to $N = r \times (k+1) = 70 \times 9 = 630$ model evaluations, where $k = 8$ is the number of screened parameters. The Sobol indices were computed using the Saltelli sampling scheme [40] with $N = 1024$ samples per parameter; bootstrap confidence intervals were subsequently estimated to quantify sampling uncertainty.

Morris screening. The Morris diagrams (Figure 8) identify the equity weight ω_3 as the dominant parameter across all outputs, with μ^* values systematically exceeding those of all other parameters. Three parameters exhibit marked non-linearity or interaction effects, appearing consistently above the diagonal $\sigma = \mu^*$: κ_2 (for $\mathcal{I}$, u_1^*, u_2^*), ω_2 (for $\mathcal{I}$, u_1^*), and κ_1 (for u_1^*, u_2^*). Notably, κ_2 exhibits the strongest interaction effects of all parameters, with $\sigma \simeq 2\mu^*$ for the inequity output, indicating that its influence on equity is highly context-dependent. In contrast, κ_1, κ_2, and κ_3 appear below the diagonal for $\mathcal{R}^*$ and Y^*, indicating predominantly linear and additive effects on these aggregate metrics. The demographic parameters N_1, N_2, N_3 cluster near the origin for $\mathcal{I}$, $\mathcal{R}$, and Y^*, confirming their marginal influence. Notably, the Morris diagrams for Y^* and $\mathcal{R}^*$ are numerically indistinguishable as confirmed by Figures 8(a) and 8(b), reflecting the exact budget identity

$$Y + \mathcal{R} = \sum_{g=1}^{G} \kappa_g u_g + \sum_{g=1}^{G} (1 - \kappa_g) u_g = \sum_{g=1}^{G} u_g = B_{\text{total}}, \tag{13}$$

which structurally couples impact and fiduciary risk in this linear model. Any efficiency–risk trade-off is therefore structurally binding rather than contingent.



(a) Impact Y^*.

(b) Risk $\mathcal{R}^*$

(c) Inequity $\mathcal{I}^*$

(d) Allocation u_1^*

(e) Allocation u_2^*

(f) Allocation u_3^*

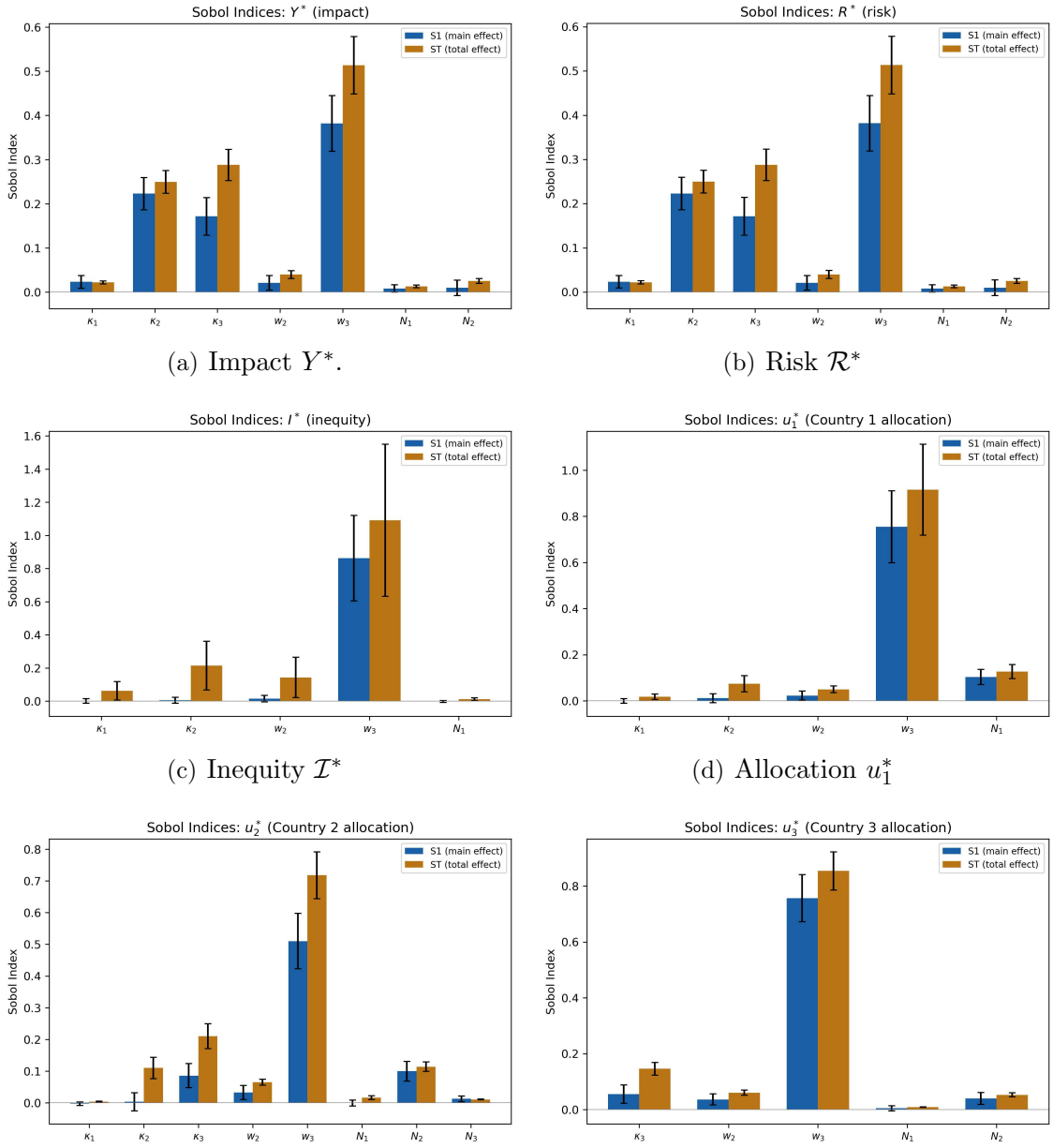
Figure 8: Morris screening (elementary effects, 70 trajectories, 630 evaluations): μ^*-σ planes for the planner's six optimal outputs. The $\sigma = \mu^*$ diagonal separates essentially additive effects (below) from strongly nonlinear or interacting effects (above).

A parameter is retained for the quantitative Sobol analysis only if it simultaneously satisfies a relative-importance criterion ($\mu_i^* \geq 10\%$ of the maximum) [34] and a statistical significance criterion (μ_i^* greater than its bootstrap confidence interval) [35]. This second criterion filters out parameters whose apparent effect is not distinguishable from sampling noise. Table 3 summarizes, for each output, the parameters retained after the combined criterion.

Output	Parameters retained for Sobol
Y^*	$\kappa_1, \kappa_2, \kappa_3, \omega_2, \omega_3, N_1, N_2$
$\mathcal{R}^*$	$\kappa_1, \kappa_2, \kappa_3, \omega_2, \omega_3, N_1, N_2$
$\mathcal{I}^*$	$\kappa_1, \kappa_2, \kappa_3, \omega_2, \omega_3, N_1$
u_1^*	$\kappa_1, \kappa_2, \kappa_3, \omega_2, \omega_3, N_1$
u_2^*	$\kappa_1, \kappa_2, \kappa_3, \omega_2, \omega_3, N_1, N_2, N_3$
u_3^*	$\kappa_3, \omega_2, \omega_3, N_1, N_2, N_3$

Table 3: Parameters retained per output after the combined criterion (relative importance $\geq 10\%$ of the maximum, and μ^* exceeding its bootstrap confidence interval). Screening performed with $r = 70$ trajectories ($N = 630$ evaluations), which ensures stable retention decisions and tight confidence intervals.

Sobol variance decomposition. The Sobol indices (Figure 9) confirm and quantify these findings. The equity weight ω_3 alone explains over 90% of the variance in $\mathcal{I}$ ($S_T = 0.94$) and approximately 80% in u_1^* and u_3^*, establishing it as the primary policy lever. For $\mathcal{R}$ and Y^*, the variance is more distributed: ω_3 contributes $S_T \approx 0.50$, followed by κ_2 ($S_T \approx 0.27$) and κ_3 ($S_T \approx 0.29$). The gap $S_T - S_1$ remains modest (typically ≤ 0.15) for all parameters, indicating that interactions, while present, do not dominate the variance structure. Population parameters exhibit $S_T \leq 0.15$ throughout, reinforcing their secondary role. The near-identity of the Sobol spectra for Y^* and $\mathcal{R}$ provides independent confirmation of the budget constraint (13). The use of $r = 70$ trajectories for Morris and $N = 1024$ samples for Sobol ensures that the reported indices are numerically converged and that the parameter ranking is stable across independent runs.



(a) Impact Y^*.

(b) Risk $\mathcal{R}^*$

(c) Inequity $\mathcal{I}^*$

(d) Allocation u_1^*

(e) Allocation u_2^*

(f) Allocation u_3^*

Figure 9: First-order (S_1, own effect) and total (S_T, own effect + interactions) Sobol indices [37, 38] for the planner's six outputs (Saltelli scheme [38], $N = 1024$), restricted to the parameter subset retained by the Morris screening for each output. Error bars: bootstrap confidence intervals.

Synthesis and implications. Three conclusions emerge from the joint Morris–Sobol analysis, summarised in Table 4. First, the allocation problem is driven more strongly by *policy preferences than by several technical parameters*: the equity weight ω_3 accounts for the majority of output variance for inequity and strongly influences the optimal allocation. This indicates that, over the parameter ranges considered, clarifying the desired balance between equity and efficiency may provide more decision-relevant information than further refinement of several technical parameter estimates. Second, the efficiency of Country 2, κ_2, functions as the system's *structural pivot*, exhibiting both substantial global influence and strong context-dependence. Its importance suggests that improved estimation of implementation efficiency in this setting warrants particular attention when characterising allocation uncertainty. Third, the budget identity (13) imposes a binding resource constraint that prevents impact and risk from being optimised independently; the resulting efficiency–risk trade-off is therefore intrinsic to the allocation problem rather than a contingent feature of a particular parameterisation. Population uncertainty, by contrast, contributes relatively little to the variation in optimal allocations over the ranges examined.

Table 4: Hierarchy of influential parameters from the joint Morris–Sobol analysis.

Rank	Parameter	Dominant role	Most affected outputs
1	ω_3	Equity policy lever (political)	$\mathcal{I}^*, u_1^*, u_2^*, u_3^*, Y^*, \mathcal{R}^*$
2	κ_2	Pivot-country efficiency (technical)	$\mathcal{I}^*, \mathcal{R}^*, Y^*, u_2^*$
3	κ_3	Low-capacity country efficiency	$\mathcal{R}^*, Y^*, u_3^*, u_2^*$
4	ω_2	Risk policy lever	$\mathcal{R}^*, u_3^*$
5	κ_1	High-capacity country efficiency	$\mathcal{R}^*, Y^*$ (weak)
6	N_1, N_2, N_3	Population sizes	u_1^*, u_2^* (weak)

The measurement priority of these parameters is high for ω_3 and κ_2, medium-high for κ_3, medium for ω_2, low-medium for κ_1, and low for N_1, N_2, N_3. Note that ω_2 and ω_3 are policy-dependent (political choices), whereas κ_2 requires empirical data collection.

5 Results and Discussion

Global health financing decisions must balance competing objectives under conditions in which resources are limited, implementation capacity varies across settings, fiduciary risks are unevenly distributed, and the benefits of financing may not accrue equally across populations. An allocation that maximizes aggregate service delivery need not minimize fiduciary exposure or reduce disparities, while an allocation

that prioritizes equity may require resources to be directed toward lower-capacity settings. These competing considerations motivate allocation approaches that make policy priorities explicit rather than treating efficiency, risk, and equity as interchangeable objectives.

The numerical experiments reported in Sections 3.3–4.3 demonstrate how these priorities shape the planner's allocation decisions. The equity weight ω_3 emerges as the parameter with the strongest influence on planner behavior, affecting the position along the Pareto frontier, the resulting allocation regime, and the trajectory of distributional inequality. The dynamic analysis further shows that a performance-based feedback rule without an explicit equity component can reinforce initial disparities, highlighting the importance of incorporating distributional considerations directly into allocation rules. The remainder of this section synthesizes these findings, discusses the limitations of the analysis, and identifies directions for future work.

5.1 Synthesis of findings

Four findings emerge from the analysis, collectively illustrating how allocation priorities, implementation capacity, and feedback mechanisms shape the balance between efficiency, fiduciary risk, and equity.

The trade-off is concave and quantifiable. The Pareto frontier in Figure 3 is concave, indicating that the initial gains in equity can be achieved with relatively small reductions in impact, whereas subsequent improvements require progressively larger efficiency sacrifices. This curvature has a direct policy implication: the marginal gain from increasing the equity weight is greatest at moderate values of ω_3 and declines as ω_3 becomes large, with diminishing returns becoming particularly evident beyond approximately $\omega_3 \approx 5$. The planner's solution under the reference weights lies on the Pareto frontier, confirming that no objective can be improved without worsening at least one of the others. By contrast, Scenarios A and B lie strictly below the frontier and are therefore dominated by alternative allocations.

Policy preferences matter more than several technical parameters. The Sobol decomposition in Figure 9 identifies the equity weight ω_3 as the dominant source of variation in inequity, with a total-order index of approximately $S_T = 0.94$, and accounts for approximately 80% of the variance in the optimal allocations u_1^* and u_3^*. For impact and risk, the variance is more distributed across ω_3 ($S_T \approx 0.50$),

κ_2 ($S_T \approx 0.27$), and κ_3 ($S_T \approx 0.29$). The relatively small differences between total-order and first-order indices indicate that interactions contribute to the variance structure but do not dominate it. These results suggest that, for the parameter ranges considered, clarifying the planner's equity preference may provide more decision-relevant information than further refining several of the technical parameters.

Country 2 is a structural pivot. The Morris analysis in Figure 8 identifies κ_2 as the most interactive parameter. For inequity, its standard deviation of elementary effects is approximately twice its mean absolute elementary effect ($\sigma \approx 2\mu^*$), indicating substantial variation in its influence across the sampled parameter space. Country 2, characterized by intermediate efficiency and population, therefore plays an important role in determining how the allocation shifts between the higher-capacity and lower-capacity countries. This result suggests that improved estimation of κ_2, together with targeted capacity-building analysis, could materially reduce uncertainty in the resulting allocation.

Performance-driven feedback can amplify disparities. The dynamic analysis in Figure 4 shows that, when the feedback rule is based solely on performance and contains no explicit equity penalty, resources increasingly concentrate in Country 1, approaching a winner-take-all allocation within approximately ten periods. The mechanism is self-reinforcing: higher initial performance attracts additional resources, which further increases subsequent performance and strengthens the allocation advantage. The result indicates that equity considerations may need to enter not only the planner's static objective but also the temporal feedback mechanism when persistent disparities are a policy concern.

5.2 Limitations and future work

Five limitations should be acknowledged. First, the production technology is linear and therefore assumes constant returns to scale, whereas absorptive-capacity constraints may generate diminishing returns as financing increases. Second, the analysis is deterministic, with uncertainty explored ex post through sensitivity analysis [41, 42] rather than incorporated directly into the optimization problem. Third, governance constraints are represented implicitly through the feasible set and fiduciary-risk penalty rather than through explicit institutional rules, enforcement mechanisms, or political constraints. Fourth, the three-country numerical experiment is intentionally stylized and cannot represent the full heterogeneity of real-world global health financing portfolios. Finally, the model has not been empirically validated

against observed allocation and service-delivery data.

Several extensions follow naturally from these limitations. First, adaptive allocation rules could be developed to incorporate observed performance over time while preventing the concentration dynamics identified in the feedback analysis; in particular, an explicit equity term could be incorporated into the feedback mechanism. Second, governance could be modeled more explicitly by introducing political-economy frictions, transaction costs, information asymmetries, and institutional constraints. Third, stochastic or robust optimization could incorporate parameter uncertainty directly into allocation decisions rather than treating uncertainty solely through ex post sensitivity analysis [35, 42]. Fourth, empirical calibration using data from major global health financing institutions could permit country-specific applications and assessment of the model against observed allocation patterns. Finally, the multilayer structure could be extended to examine how dependencies among financing, implementation capacity, governance, and service-delivery networks affect the propagation of allocation decisions across countries and population groups [7, 6].

5.3 Implications for policy

Three policy implications emerge from the analysis. First, the equity weight ω_3 is the most influential policy parameter for the distributional outcomes considered here. Explicitly defining the desired balance between equity and aggregate performance is therefore important when establishing allocation rules, particularly because moderate changes in ω_3 can substantially alter the resulting allocation. Second, the sensitivity of the allocation to intermediate-capacity settings suggests that capacity assessment and targeted capacity strengthening in such settings may have disproportionate effects on portfolio-level outcomes. Third, fiduciary risk and impact cannot generally be optimized independently: reducing exposure to fiduciary risk may require accepting lower aggregate outpu

6 Conclusion

Global health resource allocation requires decisions under competing objectives, heterogeneous implementation capacity, fiduciary risk, and unequal distribution of benefits. Treating these dimensions independently can obscure how allocation priorities interact with differences in implementation efficiency and governance-related risk. The analysis presented here formulates resource allocation as a constrained multi-objective optimization problem embedded within a multi-layer dynamical system,

linking financing flows to service delivery while accounting for implementation capacity, fiduciary risk, and distributional equity.

The numerical results quantify the resulting efficiency–equity–risk trade-off and identify the equity weight ω_3 as the dominant policy parameter for distributional outcomes. The sensitivity analysis further indicates that the problem is largely decomposable over the parameter ranges considered, while the efficiency of Country 2 acts as an important structural pivot in the allocation. The dynamic analysis shows that a feedback rule based solely on observed performance can reinforce initial differences in allocation and performance, leading to increasing concentration of resources. Together, these results indicate that equity cannot be treated solely as an ex post assessment criterion when persistent distributional disparities are a policy concern; it may also need to be incorporated directly into the allocation and feedback rules. More broadly, the analysis shows that allocation outcomes depend not only on the amount of financing available, but also on how policy preferences interact with implementation capacity, fiduciary risk, and feedback mechanisms. Making these trade-offs explicit provides a basis for examining alternative allocation rules and for identifying which assumptions and policy parameters warrant greater attention. The numerical results are illustrative rather than empirical, but the formulation provides a tractable starting point for extensions incorporating stochastic uncertainty, richer governance constraints, empirical calibration, and larger country portfolios. Such extensions could help assess whether the patterns identified here persist in more heterogeneous global health financing environments.

Declaration: The authors declare that they have no competing interest.

Ethics, Consent to Participate, and Consent to Publish declarations: not applicable.

Funding: This research received no grant from any funding agency in the public, commercial, or not-for-profit sectors.

Data availablilty: All data generated or analysed during this study are included in this published article.

CRediT authorship contribution statement: **Jean Tchuenche:** Conceptualization, Methodology, Formal analysis, Data curation, Writing – original draft,

Writing – review & editing, Validation. **Jean Pierre II Kouenkam:** Methodology, Formal analysis, Data curation, Software, Visualization, Writing – original draft, Writing – review & editing, Validation. **Herieth Rwezaura**: Methodology, Formal analysis, Data curation, Writing – review & editing, Validation. **Mamadou L. Diagne:** Methodology, Data curation, Writing – review & editing, Validation. **Joseph Mbang:** Methodology, Data curation, Writing – review & editing, Validation.

Use of Generative AI tools: ChatGPT was used to support the literature search, parameter identification, language editing, and generation of the graphical flow diagram in Figure 1, based on the mathematical model independently developed by the authors. All AI-generated outputs were independently verified against the original sources. The study design, analysis, interpretation, and conclusions were conducted solely by the authors.

References

[1] Nowzari, C., Preciado, V. M., & Pappas, G. J. (2016). Analysis and Control of Epidemics: A Survey of Spreading Processes on Complex Networks. IEEE Control Systems Magazine.

[2] Kiss, I. Z., Miller, J. C., & Simon, P. L. (2017). Mathematics of Epidemics on Networks. Springer.

[3] Bertsekas, D. P. (1995). Dynamic Programming and Optimal Control. Athena Scientific.

[4] Bertsimas, D., & Tsitsiklis, J. N. (1997). Introduction to Linear Optimization. Athena Scientific.

[5] World Health Organization (2007). Everybody's Business: Strengthening Health Systems to Improve Health Outcomes: WHO's Framework for Action.

[6] Kivelä, M., Arenas, A., Barthelemy, M., et al. (2014). Multilayer networks.*Journal of Complex Networks*, 2(3), 203–271.

[7] Buldyrev, S. V., Parshani, R., Paul, G., Stanley, H. E., Havlin, S. (2010).Catastrophic cascade of failures in interdependent networks.*Nature*, 464, 1025–1028.

[8] Lenhart, S., Workman, J. T. (2007).*Optimal Control Applied to Biological Models.*Chapman and Hall/CRC.

[9] Gini, C. (1912). *Variabilità e Mutabilità*. Bologna: Tipografia di Paolo Cuppini.

[10] Sen, A. (1973). *On Economic Inequality*. Oxford: Clarendon Press.

[11] Atkinson, A. B. (1970). On the measurement of inequality. *Journal of Economic Theory*, 2(3), 244–263.

[12] Theil, H. (1967). *Economics and Information Theory*. Amsterdam: North-Holland.

[13] Shorrocks, A. F. (1980). The class of additively decomposable inequality measures. *Econometrica*, 48(3), 613–625.

[14] Rawls, J. (1971). *A Theory of Justice*. Cambridge, MA: Harvard University Press.

[15] Bertsekas, D. P., & Gallager, R. (1992). *Data Networks* (2nd ed.). Prentice Hall.

[16] Nash, J. F. (1950). The bargaining problem. *Econometrica*, 18(2), 155–162.

[17] Kaneko, M. (1977). The Nash social welfare function. *Econometrica*, 45(2), 423–435.

[18] Kelly, F. P. (1997). Charging and rate control for elastic traffic. *European Transactions on Telecommunications*, 8(1), 33–37.

[19] World Health Organization. *Everybody's Business: Strengthening Health Systems to Improve Health Outcomes*. WHO Framework for Action, Geneva, 2007.

[20] Paina L, Peters DH. Understanding pathways for scaling up health services through the lens of complex adaptive systems. *Health Policy and Planning*. 2012;27(5):365–373.

[21] World Bank. *Improving Public Sector Performance Through Innovation and Inter-Agency Coordination*. Washington DC, 2018.

[22] The Global Fund. *Operational Policy Manual*. Geneva, Switzerland, 2023.

[23] United States Agency for International Development. *Automated Directives System (ADS) Chapter 201: Program Cycle Operational Policy*. Washington DC, 2023.

[24] Bertsekas DP. *Nonlinear Programming*. Athena Scientific, Belmont, MA, 1997.

[25] Bertsekas DP. *Dynamic Programming and Optimal Control*. Athena Scientific, Belmont, MA, 1995.

[26] Nowzari C, Preciado VM, Pappas GJ. Analysis and control of epidemics: A survey of spreading processes on complex networks. *IEEE Control Systems Magazine*. 2016;36(1):26–46.

[27] Kiss IZ, Miller JC, Simon PL. *Mathematics of Epidemics on Networks*. Springer, 2017.

[28] Rawls J. *A Theory of Justice*. Harvard University Press, 1971.

[29] Kelly FP, Maulloo AK, Tan DKH. Rate control for communication networks: Shadow prices, proportional fairness and stability. *Journal of the Operational Research Society*. 1998;49:237–252.

[30] Atkinson AB. On the measurement of inequality. *Journal of Economic Theory*. 1970;2(3):244–263.

[31] Theil H. *Economics and Information Theory*. North-Holland Publishing Company, Amsterdam, 1967.

[32] Gini C. Variabilità e mutabilità. *Studi Economico-Giuridici*. 1912;3:1–158.

[33] Morris M. D. Factorial sampling plans for preliminary computational experiments. *Technometrics*. 1991;33(2):161–174.

[34] Campolongo F, Cariboni J, Saltelli A. An effective screening design for sensitivity analysis of large models. *Environmental Modelling & Software*. 2007;22(10):1509–1518.

[35] Saltelli A, Ratto M, Andres T, Campolongo F, Cariboni J, Gatelli D, Saisana M, Tarantola S. *Global Sensitivity Analysis: The Primer*. John Wiley & Sons, Chichester, 2008.

[36] Sobol' I. M. Sensitivity estimates for nonlinear mathematical models. *Mathematical Modelling and Computational Experiments*. 1993;1(4):407–414.

[37] Sobol' I. M. Global sensitivity indices for nonlinear mathematical models and their Monte Carlo estimates. *Mathematics and Computers in Simulation*. 2001;55(1–3):271–280.

[38] Saltelli A, Annoni P, Azzini I, Campolongo F, Ratto M, Tarantola S. Variance based sensitivity analysis of model output. Design and estimator for the total sensitivity index. *Computer Physics Communications*. 2010;181(2):259–270.

[39] Campolongo F, Cariboni J, Saltelli A. An effective screening design for sensitivity analysis of large models. *Environmental Modelling & Software*. 2007;22(10):1509–1518.

[40] Saltelli, A. (2002). Making best use of model evaluations to compute sensitivity indices. *Computer Physics Communications*, 145(2), 280–297.

[41] Marino S, Hogue I. B, Ray C. J, Kirschner D. E. A methodology for performing global uncertainty and sensitivity analysis in systems biology. *Journal of Theoretical Biology*. 2008;254(1):178–196.

[42] Wu J, Dhingra R, Gambhir M, Remais J. V. Sensitivity analysis of infectious disease models: methods, advances and their application. *Journal of the Royal Society Interface*. 2013;10(86):20121018.